Acta Technica *62* (2017), No. 6B, 815–824

A damage prediction method for building structures based on convolutional neural network

Kang Deng[1], Siqi Yuan[1], Shiyu Ding[1]

Abstract. To improve the accuracy on structural damage prediction of Kashgar high platform folk house, put forward a kind of prediction method for structural damage of Kashgar high platform folk houses based on convolution neural network (CNN). Firstly, utilize the dynamic characteristic equation of free vibration for many degrees of freedom system, give the theoretical basis model for damage analysis of Kashgar high platform folk houses, and explain the correlation between frequency change of free order and damage information of structure; then, introduce the convolution neural network to predict the structural damage of Kashgar high platform folk houses, as CNN network is operated in the little image window during the training and testing stage, enabling the network weight to observe the feature of high platform folk houses from the input data via this window; finally, through the simulation experiment analysis, verify the efficiency of raised algorithm.

Key words. Convolution neural network, Kashgar high platform folk houses, Structural damage, Free vibration.

1. Introduction

The guiding concept for old Kashgar city reconstruction is to put the life safety in the first place, and combine the unsafe houses reconstruction in old city with earthquake prevention, especially the reconstruction against the high platform folk houses; combine it with the aid to the poor and improvement of resident life; combine with tradition and promotion of Uyghur historical culture; combine with the long-term urban development. In the concrete implementation process, apply the site renovation, extensively solicit the resident wishes, and design door by door, with resident participating in the implementation during the construction process, especially the roof, railing, stairs, column type, window and door during the decoration at the later stage.

[1]School of Civil Engineering & Architecture, Nanchang University, Nanchang, 330031 China

During long-term use, gone through the aging or influenced by the earth, typhoon and other factors, the building structure would be affected by the damage in different degree. At the present, many methods in the data mining are applied into the identification field of building structural damage, mainly including the neural network, support vector machine and other machine learning algorithms. Literature [5] researches the damage detection on main girder structure of steel bridge with artificial neural network and finite element model, result showing: the artificial neutral network after acquired valve sample training has the strong potential advantage in the structural damage identification. Literature [6] researches the applicability of Bayesian neural networks in the structural damage identification of cable stayed bridge. Literature [7] positions the structural damage with cepstrum analysis and response measured value obtained by artificial neural network. As the wavelet analysis has the analytical ability on signal multi-resolution and time-frequency localization nature, combination with advantages of wavelet analysis and neural network is able to further develop the structural damage identification theory.

Based on the above algorithms, aiming at the decision on structural damage of Kashgar high platform folk houses, with the convention neutral network as the analysis tool, this paper designs the analysis algorithm for the structural damage prediction and verifies the efficiency of raised method through the experiment.

2. Theoretical basis

2.1. Structure of Kashgar high platform folk houses

The Uyghur name of high platform folk house is Kuoziqiyabeixi Lane, referring to the Gaoya Earthenware, named from the millennial pottery process, as shown in Fig.1. The high platform folk houses are built on the loess high cliff for more than 20m high and 400m long at the southeast end of old city, adjoining to Tuman River and East Lake Park. As most of existing residences are established after the great earthquake in 1902, the old houses for hundred years are everywhere. Most residents are Uyghur, mainly working on the traditional Uyghur handicraft manufacture. Here, the ethnic characteristics and life features are intensively reflected, showing the unique charm.

2.2. Structural damage theory

For any many degrees of freedom system, the dynamic characteristic equation of its free vibration can be expressed as:

$$M\ddot{d} + C\dot{d} + Kd = 0\,. \tag{1}$$

In the formula, d is the displacement vector for degree of freedom of node, $\dot{d}$ and $\ddot{d}$ respectively as the first and second derivative of d to the time, namely the velocity vector and acceleration vector of node. M is the system mass matrix, C as the system damping matrix and K as the systematic stiffness matrix. Leaving out

Fig. 1. Kashgar high platform folk houses

the damping influence, simplify the Formula (1) as

$$M\ddot{d} + Kd = 0\,. \tag{2}$$

The Formula (2) is called as the system non-damping free vibration equation. As each point makes the simple harmonic vibration nearby the equilibrium position when free vibration, $d = \phi sin\omega(t - t_0)$, then, its characteristic equation can be represented as:

$$(K - \omega^2 M)\phi = 0\,. \tag{3}$$

In the formula, K and M respectively are the global stiffness matrix and mass matrix; φ is the regularization vibration mode; ω is the inherent frequency. Assuming that the damage causes certain change to the structural stiffness matrix and mass matrix, then, corresponding changes shall be made to φ and ω, and the structural motion equation after damaging is:

$$[(K + \Delta K) - (\omega^2 + \Delta\omega^2)(M + \Delta M)](\phi + \Delta\phi) = 0\,. \tag{4}$$

In the formula: ΔK, ΔM, $\Delta\varphi$ and $\Delta\omega$ respectively are the global stiffness matrix, mass matrix, vibration mode and frequency variations. The damage position and degree of engineering structure normally have obvious influence to the stiffness matrix of structure, with relatively small influence to the mass distribution. Therefore, ΔM can be left out. Leave out ΔM in the Formula (4) and expand as follows:

$$\Delta\omega^2 = \frac{\phi^T \Delta K \phi}{\phi^T M \phi}\,. \tag{5}$$

For one pure vibration mode $i(i = 1, 2, \cdots)$, then:

$$\Delta\omega_i^2 = \frac{\phi_i^T A K \phi_i}{\phi_i^T M \phi_i}\,. \tag{6}$$

The total stiffness matrix of structure can be divided into the element stiffness matrix, while the element deformation can be calculated from the vibration mode

of structure, namely:

$$\varepsilon_m(\phi) = f(\phi)\,. \tag{7}$$

In the formula, ε_m is the element number, and m is the element deformation. Then:

$$\phi_i^T K \phi_i = \sum_{m=1}^{M_1} \varepsilon_m^T(\phi_i) k_m \varepsilon_m\,. \tag{8}$$

In the formula, M_1 is the sum of structural element. There is:

$$\phi_i^T \Delta K \phi_i = \sum_{m=1}^{M_1} \varepsilon_m^T(\phi_i) \Delta k_m \varepsilon_m(\phi_i)\,. \tag{9}$$

Then, the Formula (6) can be transformed as:

$$\Delta\omega_i^2 == \frac{\sum\limits_{m=1}^{M_1} \varepsilon_m^T(\phi_i) \Delta k_m \varepsilon_m(\phi_i)}{\phi_i^T M \phi_i}\,. \tag{10}$$

For the single damage element N of building structure, the Formula (10) can be simplified as:

$$\Delta\omega_i^2 = \frac{\varepsilon_N^T(\phi_i) \Delta k_N \varepsilon_N(\phi_i)}{\phi_i^T M \phi_i}\,. \tag{11}$$

From the Formula (11), it can be known that: the change to structural frequency is directly linked to the element change. The structural frequency change in free order contains the damage degree information of same element N. The change to natural frequency and modal shape caused by the damage in one position can be taken as the identification index for specific damage.

3. Convolution neural network prediction

3.1. Establishment of network mapping

In the pattern identification algorithm based on CNN network, it is required to represent the input data as the feature mapping form. Represent the input data as the input of 2D array, presenting in the horizontal x and vertical y pixel form. CNN network operates in the small window for inputting image during the training and testing stage, enabling the network weight to observe the feature of high platform folk houses from the input data via this window.

At the present, there are many types of input forms of DNN matrix. In this case, 2D convolution operation can be carried out, while the normalization operation can be carried out for the frequency and time at the same time. Or, only take the frequency normalization here. In such case, the same features of high platform folk houses are combined as the 1D feature mapping. Once constructing the input feature vector, respectively activate the operation in the convolution and convergence layer.

Similar to input layer, the convolution and convergence layer of the element also can be expressed as the mapping matrix form. In the CNN terms, the convolution and convergence layer can be expressed 1 CNN layer.

3.2. CNN convolution layer

As shown in Fig.1, for every input feature mapping, assuming that I is the total quantity of mapping, $O_i(i = 1, \cdots, I)$; connecting to multiple feature mapping (assuming that the total quantity is J), $Q_j(j = 1, \cdots, J)$; the convolution layer based on local weight matrix is $I \times J$, $w_{i,j}\,(1, \cdots, I; j = 1, \cdots, J)$. The mapping can be expressed as the convolution calculation in the signal processing. Assuming that the input feature mapping is 1D, the feature mapping for convolution layer of every nerve cell can be calculated as:

$$q_{j,rm} = \sigma\left(\sum_{i=l}^{I}\sum_{n=1}^{F} o_{i,n+m-1}w_{i,j,n} + w_{o,j})\right),\ (j = 1, \cdots, J)\ . \tag{12}$$

In the formula, $o_{i,m}$ is the ith input for feature mapping O_i of nerve cell m; is the jth input for nerve cell m of convolution layer feature mapping O_j; is the nth element of weight vector$w_{i,j}$; F is the filter size, with its value determining the number of feature mapping band input by every convolution layer.

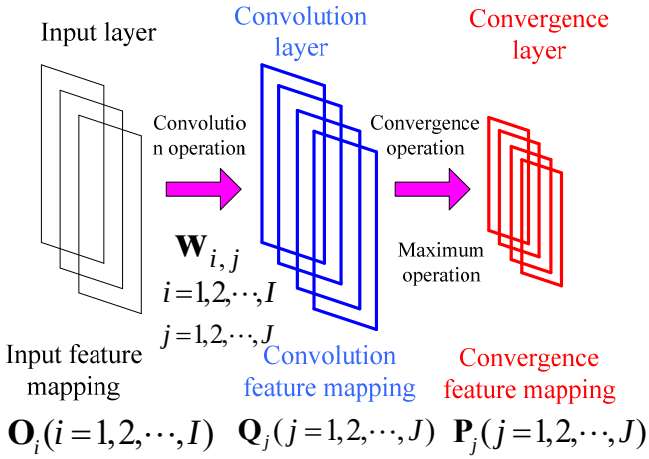

Fig. 2. CNN network operating structure

Because of the localized feature mapping of selected high platform folk house, these feature mappings are defined within the limited signal feature range of high platform folk houses. Based on the convolution operator, the Formula (8) can be simplified in matrix form:

$$Q_j = \sigma(\sum_{i=1}^{I} O_i * w_{i,j}),\ (j = 1, \cdots, J) \tag{13}$$

In the formula, O_i represents the ith input feature mapping, and $w_{i,j}$ represents the localized weight matrix. When on the basis of 1D feature mapping, O_i and $w_{i,j}$ are vectors; when on the basis of 2D feature mapping, O_i and $w_{i,j}$ are the matrixes.

3.3. CNN convergence layer

As shown in Fig.2, exert the convergence operation in the CNN convergence layer to generate the corresponding convergence layer. The convergence function is independently applied to every convolution feature mapping. When using the maximum convergence function, CNN convergence layer can be defined as [14]:

$$p_{i,m} = \max_{n=1}^{G} q_{i,(m-1)\times s+n} \,. \tag{14}$$

Of which, G is the scale of convergence layer, and s is the displacement size, determining the contact ratio of adjacent convergence windows. Similarly, if using the mean function, then, the output can be calculated as:

$$p_{i,m} = r \sum_{n=1}^{G} q_{i,(rm-1)\times s+n} \,. \tag{15}$$

In the formula, r is the scale factor able to be studied. Normally, in the image identification application, under the constraint $G = s$, in case of no overlap of convergent window, there is no clearance among them. In this condition, the maximum convergence feature mapping is showed to be superior to the mean convergence feature mapping. In this paper, independently adjust G and s. In addition, apply the nonlinear activation function to generate the final output. The schematic diagram of convergence process with convergence layer size of 3 is given in the Fig.2. Every convergence layer element accepts the nerve cell input of three convolution layers in the same feature mapping. If $G = s$, then the convergence layer size will be one third of convolution layer size.

4. Experimental analysis

4.1. Structural damage simulation and acquisition of response signal

Most researches on structural damage detection method begin from the numerical simulation, which refers to the damage simulation method. Normally, for small damage, only the change to structural stiffness shall be considered when simulating, dispense with considering the change to mass. The simplest simulation method is to build the finite element model of structure, and simulate the structural damage for lowering the stiffness of one element. The quantitative range of small damage can be deemed as the product of reduction ratio of element stiffness and proportion of element size occupying the overall structure size. The relation between the percent ratio of stiffness reduction and actual physical damage mode shall be deter-

mined according to the actual structural materials. The research with great difficulty belongs to the microscopic damage mechanics category, while its corresponding relation being referred to the "finite element modeling method of improved small damage mechanics".

In the project practice, as the bridge structure will normally be affected by random exciting load when various vehicles pass during the using process, the random accelerated speed is considered to be exerted, the oscillogram as shown in Fig.4.

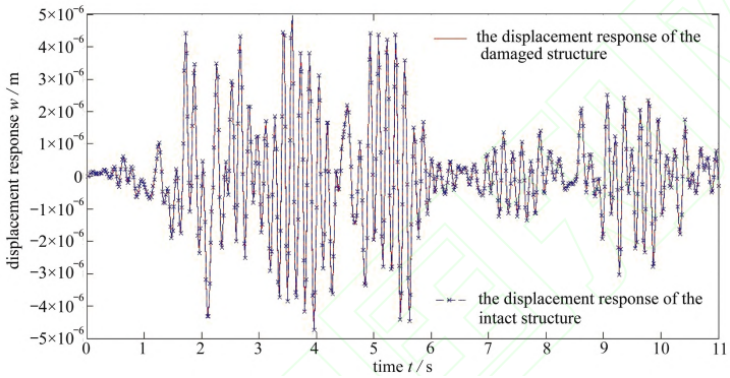

Fig. 3. Displacement response signals of intact structure and damage structure

Then, predict and analyze the bridge structure with CNN network, and extract the displacement response signal. The Fig.4 is the comparison diagram of displacement response signal for damage structure state and intact structure. From the Fig.3, it can be seen: the displacement response before and after damage has no obvious change.

4.2. Damage detection result

When training facing to all plate elements, the selected training samples are: plate element 8, 25, 44, 52, 55, 63, 73, 76, 82, 90, 97, 108, 120, 127, 134, 140, 144, 150, 159, 163, 186, 194, 209, 216, 222, 232, 236, 238, 245, 251, 254, 264, 269, 280, 283, 288, 299, 301, 307, 312, 315, 321, 326, 333, 337, 351, 357, 371, 388 and 392 (totally are 50 elements), respectively damages for 0.0124%, 0.0187%, 0.0218%, 0.0342% and 0.0404% and so that can construct total 250 single damage operating conditions. See Fig.9 for the concrete position. The selected 9 test samples are No.63 plate element (damage for 0.0311%), No.150 plate element (damage for 0.0311%) and No.283 plate element (damage for 0.0311%); No.108 plate element (damage for 0.0280%), No.216 plate element (damage for 0.0280%) and No.301 plate element (damage for 0.0280%); No.44 plate element (damage for 0.0155%), No.186 plate element (damage for 0.0155%) and No.337 plate element (damage for 0.0155%). At this moment, the neural network has 250 training samples and 9 testing samples. After applying the Matlab initialization network, carry out the training and obtain the network error of 0.0433, illustrating that the network training is efficient. Input the testing sample into the trained network, the output result as shown in Table 1.

Table 1. Detection result for neural network of training deck slab

board element number	damage degree B/%	actual coordinate X	Y	Z	network output coordinate X	Y	Z	maximum error δ_m/%
63	0.031 1	0.25	2.35	1.00	0.244 2	2.358 4	1.000 1	2.32
150	0.031 1	0.45	3.05	1.00	0.467 7	2.906 8	1.000 0	3.93
283	0.031 1	0.85	0.35	1.00	0.837 9	0.311 2	0.999 9	3.88
108	0.028 0	0.35	2.85	1.00	0.336 5	2.993 6	1.000 0	5.03
216	0.028 0	0.65	1.65	1.00	0.692 3	1.658 8	1.000 0	6.51
301	0.028 0	0.85	2.15	1.00	0.813 5	2.146 8	1.001 0	4.29
44	0.015 5	0.25	0.45	1.00	0.254 4	0.482 0	1.000 0	7.11
186	0.015 5	0.55	2.65	1.00	0.569 9	2.402 4	1.000 0	9.34
337	0.015 5	0.95	1.75	1.00	0.865 0	1.695 0	1.000 0	8.95

From the Table 1, it can be seen that, for the damage positioning result of testing sample, the maximum error is less than 9.34%; when in great damage, if the damage is 0.0311% and 0.028%, the maximum positioning error is less than 6.51%, with better effect than when damage is 0.0155%. This is because the greater the damage is, the greater the caused difference response signal, and the more obvious the change to damage characteristic quantity is. When training only facing to the plate, the network is convergent, with good damage positioning ability.

5. Conclusions

The damage to building structure is an important problem in connection to building safety. To identify the damage position and degree of building structure, set up the model against the actual engineering building structure, take the natural frequency change rate of building structure as the damage index, and identify the different damage condition of building structure by utilizing the neural network technology. The result of simulation test shows that, application of the frequency change ratio as the convolution neural network of input vector can well identify the damage degree of components, with its relative error of identification being controlled within 3%.

The method can position the damage position to the resident position, to provide the reference basis for the online monitoring and damage identification and prediction of complex building structure, and to further lay a theoretical and method basis for achieving the adoption of frequency test method and evaluation of healthy condition of building structure in the actual building structure.

References

[1] Wang C, Yang D, Pang F: (2014) *Study on tunnel safety incipient danger and countermeasures optimization in high-terrace folk house in Kashgar city*[J]. Journal of Chemical & Pharmaceutical Research.

[2] Hayslett J P, Kashgarian M, Epstein F H: (1968) *Functional correlates of com-*

pensatory renal hypertrophy.[J]. Journal of Clinical Investigation, , 47(4):774-99.

[3] Hayslett J P, Kashgarian M: (1979) *A micropuncture study of the renal handling of lithium.*[J]. Pflügers Archiv - European Journal of Physiology, 380(2):159-63.

[4] Wang T: (1995) *Effects of chronic hyperfiltration on proximal tubule bicarbonate transport and cell electrolytes.*[J]. Kidney International, 48(3):712-21.

[5] Dennis V W: (1976) *Influence of bicarbonate on parathyroid hormone-induced changes in fluid absorption by the proximal tubule.*[J]. Kidney International, 10(5):373-80.

[6] Bartoli E, Earley L E: (1971) *The relative contributions of reabsorptive rate and redistributed nephron filtration rate to changes in proximal tubular fractional reabsorption during acute saline infusion and aortic constriction in the rat.*[J]. Journal of Clinical Investigation, 50(10):2191-203.

[7] Hirsch D, Kashgarian M, Boulpaep E L, et al.: (1985) *Role of aldosterone in the mechanism of potassium adaptation in the initial collecting tubule*[J]. Kidney International, 26(6):798-807.

[8] Silbernagl S, Völkl H, Vetter G: (1977) *Amino acid reabsorption in the proximal tubule of rat kidney: Stereospecificity and passive diffusion studied by continuous microperfusion*[J]. Pflügers Archiv - European Journal of Physiology, 367(3):221-227.

[9] Boyd S, Chua L: (1985) *Fading memory and the problem of approximating nonlinear operators with Volterra series*[J]. IEEE Transactions on Circuits & Systems, 32(11):1150-1161.

[10] Arp G, Thiel V, Reimer A, et al.: (1999) *Biofilm exopolymers control microbialite formation at thermal springs discharging into the alkaline Pyramid Lake, Nevada, USA*[J]. Sedimentary Geology, 126(1–4):159-176.

[11] Klauser D, Coish W A, Loss D: (2006) *Nuclear spin state narrowing via gate–controlled Rabi oscillations in a double quantum dot*[J]. Physical Review B, 73(20):5302.

Received May 7, 2017